

# Simultaneous detection of hydroquinone and catechol on electrochemical-activated glassy carbon electrode by simple anodic and cathodic polarization

Hua Zhang<sup>1,2</sup> · Sue Li<sup>1</sup> · Fenghua Zhang<sup>1</sup> · Meixia Wang<sup>1</sup> · Xiuchong Lin<sup>1</sup> · Huaixiang Li<sup>1</sup>

Received: 14 September 2016 / Revised: 30 September 2016 / Accepted: 3 October 2016 / Published online: 11 October 2016  
© Springer-Verlag Berlin Heidelberg 2016

**Abstract** Herein, we report a simple method of simultaneous detection of hydroquinone (HQ) and catechol (CC) by cyclic voltammetry (CV) using activated glassy carbon electrodes (GCE). It was found that the two isomers can be completely separated by CV method on cathode polarized GCE (PGCE) after its anodic oxidation. This facile processing method solves the difficulty of electrode surface regenerating which disturb most modified electrodes for the complex composition ease of being contaminated by the analytes in measurement. Morphology and composition of the PGCE were characterized by scanning electron microscope (SEM), Fourier transform infrared (FTIR) spectra, and X-ray photoelectron spectroscopy. In addition, the reaction kinetic of HQ and CC reaction on the PGCE was investigated. It was found that the reaction kinetics of HQ and CC is a surface adsorption-controlled process at low concentration and a diffusion-controlled process at high concentration.

**Keywords** Catechol · Hydroquinone · Simultaneous detection · Cyclic voltammetry · Polarized glassy carbon electrode

## Introduction

Detection of hydroquinone (1,4-dihydroxybenzene, HQ) and catechol (1,2-dihydroxybenzene, CC) has long been an important work of analytical chemistry researchers for their toxicity to human and animals in the environment [1]. The absorption of dihydroxybenzene may cause some disease like renal tube degeneration and liver function decrease [2]. So it is necessary to develop sensors to detect and monitor the concentration of dihydroxybenzene. Detection of HQ and CC is based on the physical and chemical properties of the dihydroxybenzene. Owing to the similarity of the two isomers, it is difficult to distinguish one from the other in most cases. In recent years, many techniques have been tried to distinguish the two isomers such as traditional high-performance liquid chromatography (HPLC) [3, 4] and electrochemical methods [5, 6]. HPLC is a mature and reliable technique in substance separation and detection but suffers from expensive cost and long-time testing. In comparison, electrochemical methods have the advantage of high efficiency, low cost, and ease of use. In recent years, many new composite materials, such as carbon nanomaterial [7–9], metal oxides [10], metal nanoparticles [11, 12], and conducting polymers [13, 14] have been used to fabricate modified glassy carbon electrode (GCE) for the electrochemical determination of dihydroxybenzene isomers. These modifications either reduce the overpotential or increase the sensitivity and selectivity of the electrodes. Although many literatures have been reported in simultaneous detection of HQ and CC [15–21], they mainly focus on the function of modification materials. However, the modification materials are ease of falling off and contaminated by some components in the measurement solution, which resulted in long-term instability or loss of sensitivity [22]. We also

✉ Huaixiang Li  
lihuaixiang@sdu.edu.cn; lihuaixiang1212@163.com

<sup>1</sup> College of Chemistry, Chemical Engineering and Materials Science, Collaborative Innovation Center of Functionalized Probes for Chemical Imaging in Universities of Shandong, Key Laboratory of Molecular and Nano Probes, Ministry of Education, Shandong Provincial Key Laboratory of Clean Production of Fine Chemicals, Shandong Normal University, Jinan 250014, People's Republic of China

<sup>2</sup> School of Materials Science and Engineering, Shandong University of Technology, Zibo 255000, People's Republic of China

noticed that many modification materials are carbon material, such as graphene and doped graphite materials.

Glassy carbon electrode (GCE) is a popular electrode in electroanalysis for its wide potential range, inexpensive, readily available, and chemically inert properties in most electrolytes [23]. Concerning glassy carbon is also a carbon material which mainly comes from the destructive distillation of polyacrylonitrile resin or phenolic resin; GCE also has the application potential like the other carbon materials mentioned above. To meet the special electrochemical measurement, many techniques, such as mechanical polishing [24], reduced pressure heating [25], hot filament technique [26], laser irradiation [27], hydrogen plasma [28], and electrochemical activation [29–32], have been developed to active GCE. In comparison, electrochemical disposal is a simple, facile, and highly repeatable method in electrode treatments [33] and appropriate solvation may trigger its electrochemical activity. If this assumption is validated, it would greatly simplify the progress of sensitive electrode modification.

From the view of electrochemical detection, cyclic voltammetry (CV) is a popular and widely used technique in electrochemical analysis for the abundant information, such as the reversibility of an electrochemical reaction, the concentration of the analytes and even the electron exchange coefficient in some cases. Many other electrochemical measurements, such as differential pulse voltammetry (DPV) and chronoamperometry, are all based on the chemical reactions of analytes on electrode at different potentials. Although each has its own characteristics, e.g., DPV is more sensitive in current signal recognition and chronoamperometry is a more direct and continuous measurement, there are no essential difference between the electrochemical measurements that based on the detection of Faraday current. For simplicity, CV measurement was used to study the fundamental process of electron transition between the electrode surface and species (either molecules or ions) in the electrode/solution interfacial region.

In this work, an electrochemically polarized glassy carbon electrode (PGCE) was employed to differentiate HQ and CC by CV method. Experimental results indicated that the two isomers of dihydroxybenzene can be differentiated by the PGCE from the redox peaks on the CV curves. This electrochemical polarization is a simple, rapid, highly repeatable, and sensitive method for detection of HQ and CC. Furthermore, it prevents the difficulty of regenerating the sensing interface, which fouls the electrode surface by adsorbed HQ and CC during measurement on the most modified electrodes. The polarization process proceeds under the same experimental solution (pH = 7.0 PBS) as the determination of HQ and CC, which provides great convenience in measurements.

## Experimental

### Materials and chemicals

Commercial glassy carbon electrodes (GCE, 3 mm in diameter) were obtained from Bioanalytical Systems, Inc. (West Lafayette, IN, USA). Hydroquinone (1,4-dihydroxybenzene, HQ), catechol (1,2-dihydroxybenzene, CC)  $K_2HPO_4$  and  $KH_2PO_4$  were purchased from Shanghai Chemical Reagent Factory (China). All the chemicals were of analytical grade without further purification. Solutions were prepared with doubly distilled water obtained from a Milli-Q water purifying system ( $>18\text{ M } \Omega\text{ cm}$  at 293 K). Phosphate buffer solution (0.1 M PBS, pH = 7) was prepared by  $K_2HPO_4$  and  $KH_2PO_4$  with KCl as supporting electrolyte.

### Electrochemical polarization and measurements of GCEs

Polarization (anodization or cathodization), cyclic voltammetry (CV), chronoamperometry experiments and electrochemical impedance spectra (EIS) were performed using a CHI-660D electrochemical workstation (CHI Inc. Ltd., Shanghai) coupled with a conventional three-electrode cell. The GCE and the polarized GCEs were used as the working electrodes with a platinum plate as auxiliary electrode and a saturated calomel electrode (SCE) as reference electrode. GCEs were polished with 0.3- and 0.05- $\mu\text{m}$  alumina slurry and then cleaned ultrasonically in double distilled water and ethanol successively. The polarization conditions are optimized by changing the potential or polarization time in pH 7 PBS. A freshly polished electrode anodized at 1.70 V for 20 min and then cathodized at  $-1.00\text{ V}$  for 15 min was found to be the optimally polarized electrode, abbreviated as PGCE and used for electrochemical measurements.

### Characterization of samples

The morphology of the polarized electrode was observed by scanning electron microscope (FEI Quanta 250, USA) with a field emission gun operating between 200 and 20 kV in a vacuum with resolution of 3.0 nm at 30 kV and 8.0 nm at 3 kV. Fourier transform infrared (FTIR) spectra were recorded on a Bruker tensor 27 Fourier transform infrared spectrometer. The spectra were measured in the  $4000\text{--}400\text{ cm}^{-1}$  wave number range. X-ray photoelectron spectroscopy (XPS) was used to determine film composition on a Perkin Elmer PHI-5600 system using monochromatic Al  $K\alpha$  radiation (1486.6 eV). The X-ray generator was operated at 250 W (12.5 kV). The specimens were analyzed using a spherical capacitance analyzer at an electron take-off angle of  $45^\circ$ . The analyzer energy resolution (the energy difference between two recorded data points) was 0.4 eV for survey scans and 0.1 eV for multiplex

scans. The peak positions were calibrated against the carbon 1 s peak at 284.6 eV.

## Result and discussion

### Results of characterization

The morphology of the GCE before and after anodic/cathodic treatment was examined by SEM. Figure 1a shows the SEM image of bare GCE with a flat surface. By comparison, shown as in Fig. 1b, a bumpy surface could be observed on the PGCE after electrochemical treatment by cathodizing at  $-1.0$  V for 15 min after anodizing at  $1.7$  V for 20 min. The result is consistent with the previous report that potentiostatic activation produced larger void space in the interior of the activated film to accommodate adsorbents of larger sizes [34].

FTIR spectra of the GCE and PGCE are depicted in Fig. 2. The blue solid line shows the FTIR spectrum of the GCE and the red dash line shows the FTIR spectrum of the PGCE. As can be seen, there are great differences between the GCE and PGCE. The strong wide band centered at about  $3300\text{ cm}^{-1}$  in the PGCE spectrum is corresponded to the stretching vibration of the associated O–H bond ( $\sigma_{\text{O-H}}$ ) in carboxyl group ( $-\text{COOH}$ ). Owing to the conjugative effect, the stretching vibration of C=O bond ( $\sigma_{\text{C=O}}$ ) in carboxyl shifts from typical  $1760\text{ cm}^{-1}$  [35] to low wavenumber of about  $1725\text{--}1700\text{ cm}^{-1}$  in conjugative state, corresponding to the sharp strong peak at  $1710\text{ cm}^{-1}$  in the PGCE spectrum. The peaks at about  $1200\text{ cm}^{-1}$  in the PGCE spectrum are ascribed to the stretching vibration of C–O bond ( $\sigma_{\text{C-O}}$ ) in tertiary alcohol and the flexural vibration of O–H bond ( $\delta_{\text{O-H}}$ ) in hydroxyl group [36]. As to the multiple peaks at about  $2500\text{ cm}^{-1}$ , no typical function groups are traced. They might be the double frequency absorption of  $\sigma_{\text{C-O}}$  and  $\delta_{\text{O-H}}$  which have been analyzed at the  $\sim 1200\text{ cm}^{-1}$ . The results indicate that abundant hydroxyl groups and carboxyl groups generated after the GCE being electrochemically disposed to be PGCE and the hydroxyl and carboxyl groups may greatly enhance the electrochemical activity of the PGCE.

**Fig. 1** SEM images of GCE (a) and PGCE (b)

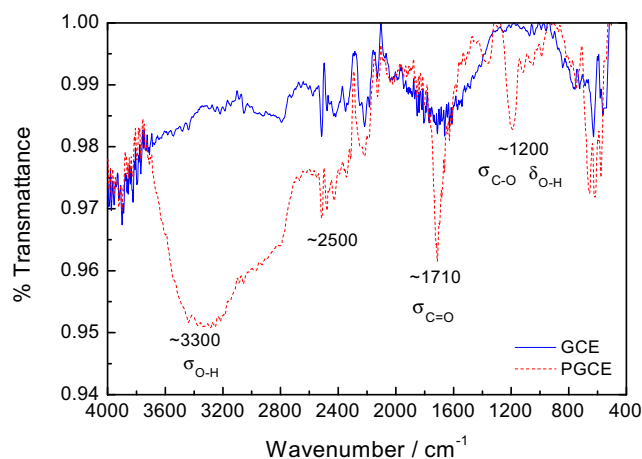
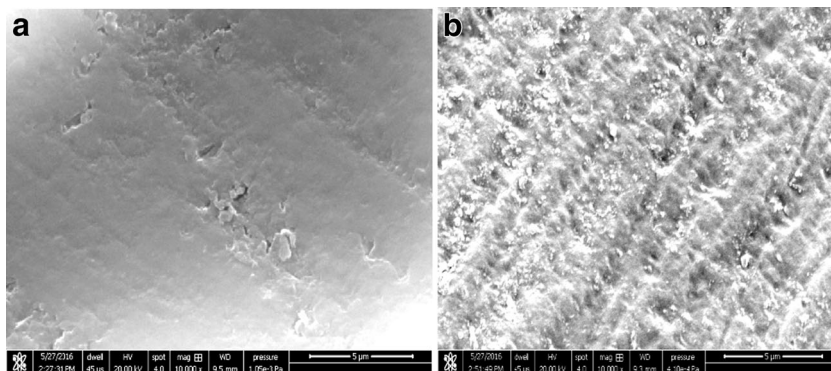


**Fig. 2** FTIR spectra comparison of the GCE and the PGCE

The surface of GCE and PGCE were further examined by XPS measurement. No signal from phosphorus was detected at the surface of the PGCE, indicating that phosphate anions in the supporting electrolyte were not adsorbed on the activated electrode during the polarization process. Figure 3A shows a decrease (from curve a to curve b) in amplitude of C1s peak after the polarization, but the O1s peak amplitude in Fig. 3B increases from the GCE (curve a) to the PGCE (curve b), although the peak shape changed a little. Calculations based on the peak area indicate that the oxygen-to-carbon ratio of the electrode surface were 0.17 and 0.27 for the GCE and the PGCE, respectively. The increase in the O/C ratio and the increase of O1s peak amplitude show that the surface became oxygenated during polarizing process, which is similar to the results reported by others [37]. The O/C states in the PGCE were studied by means of peak-differentiation-imitating analysis, and relative results were showed in Fig. 3C and Fig. 3D. Figure 3C presents the deconvolution of the C1s signal from the PGCE sample. The three peaks (dash line derived from the solid line) with binding energy at about 284.6, 286.5, and 288.5 eV indicate the presence of different forms of carbon, such as carbonyl, carboxyl, and quinone [38]. The O1s peak for PGCE in Fig. 3d was deconvoluted into three parts located at 529.2, 531.1, and 533.3 eV, corresponding to O–H, C=O

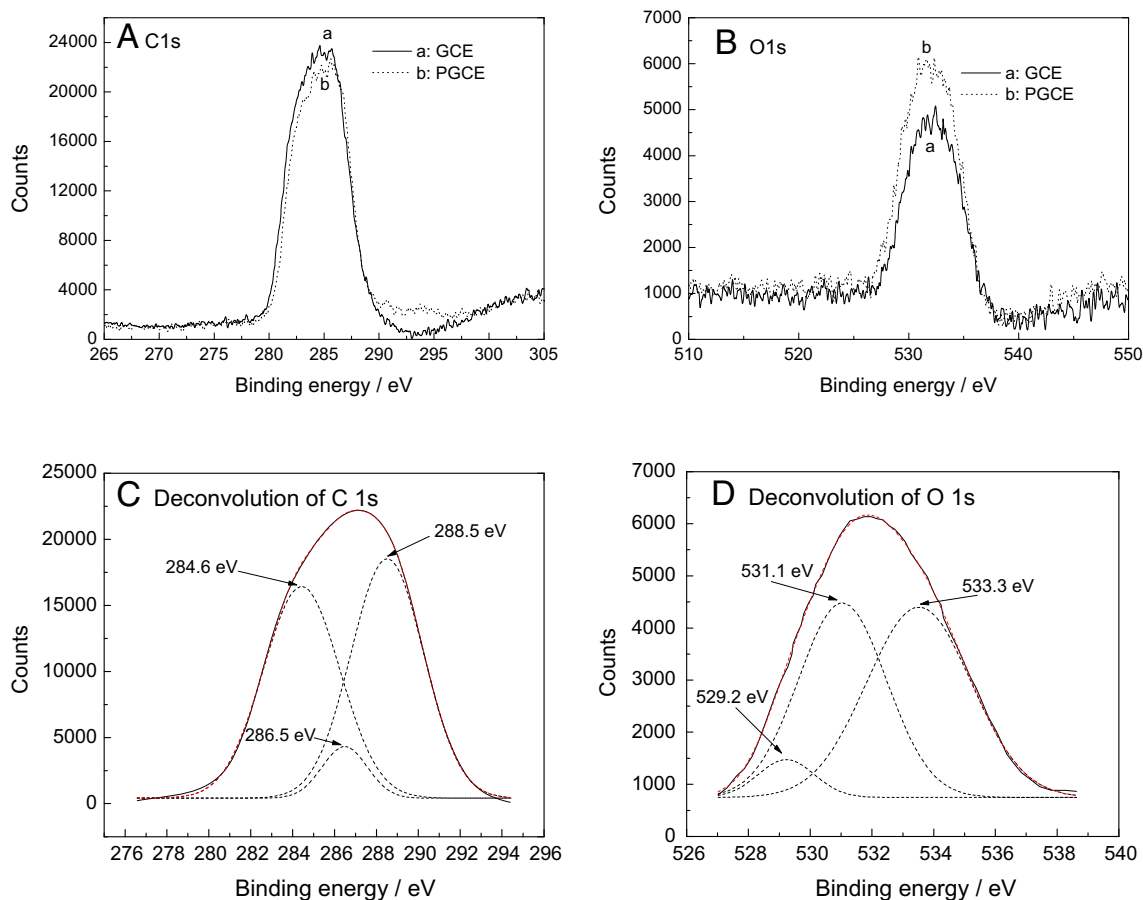


**Fig. 3** **A** C1s, **B** O1s XPS spectra of GCE (*a*: solid) and PGCE (*b*: dotted), **C** deconvolution of C1s spectra of the PGCE and **D** deconvolution of O1s spectra of the PGCE

and C–O [39], respectively, which are consistent with the results of FTIR spectra in Fig. 2.

By using 20 mM  $\text{K}_3\text{Fe}(\text{CN})_6/\text{K}_4\text{Fe}(\text{CN})_6$  as redox probe, we investigated the charge transfer properties of the polarized electrodes at the solution/electrode interface in 0.10 M KCl solution. The cyclic voltammograms (CVs) of unpolarized GCE (curve *a*) show a pair of redox peaks, and the CVs of the PGCE (curve *b*) display higher peak currents, as seen in Fig. 4A. The difference between the two curves can be

attributed to the later having larger electroactive surface areas. The electroactive surface area of the electrode can be calculated according to the Randles-Sevcik equation [40]:

$$I_p = 2.69 \times 10^5 A D^{1/2} n^{3/2} \nu^{1/2} C \quad (1)$$

where  $A$ ,  $D$ ,  $n$ ,  $\nu$ , and  $C$  is the area of the electrode ( $\text{cm}^2$ ), diffusion coefficient of the molecule ( $\text{cm}^2/\text{s}$ ), number of electron transfer in the redox reaction, scan rate ( $\text{V}/\text{s}$ ) and

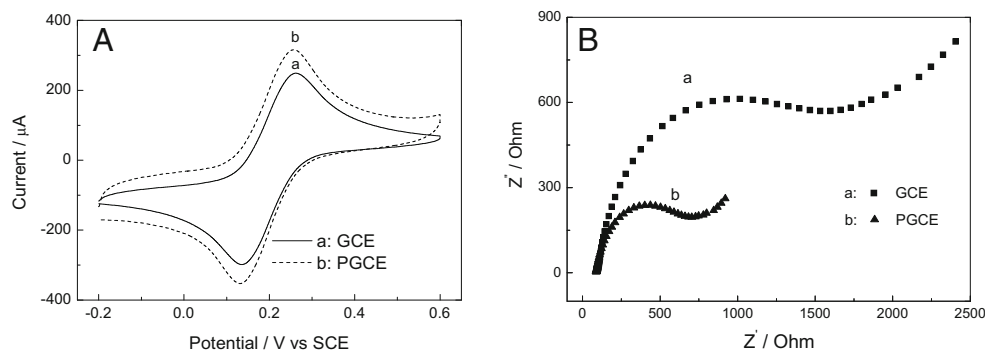


**Fig. 4** **A** Cyclic voltammograms recorded at GCE (*a*) and PGCE (*b*) for 20 mM  $\text{K}_3\text{Fe}(\text{CN})_6/\text{K}_4\text{Fe}(\text{CN})_6$  in 0.10 M KCl solution at scan rate of  $0.02 \text{ V s}^{-1}$ . **B** Nyquist plots of EIS of GCE (*a*) and PGCE (*b*) in 20 mM

$\text{K}_3\text{Fe}(\text{CN})_6/\text{K}_4\text{Fe}(\text{CN})_6$  contains 0.10 M KCl solution at the applied frequency range of 0.05 Hz–100 kHz

**Fig. 5** Influence of cathodization (A) and anodization (B) on characteristics of 500 μM HQ and 500 μM CC in 0.1 M PBS (pH 7.0) at 50 mV s<sup>-1</sup> scan rate. A For (a) 0 min, (b) 5 min, (c) 10 min, (d) 15 min, (e) 20 min after anodizing at 1.7 V for 20 min. B At (a) 0.8 V, (b) 1.1 V, (c) 1.4 V, (d) 1.7 V, (e) 2.0 V and then cathodized at -1.0 V for 15 min, (f) unpolarized

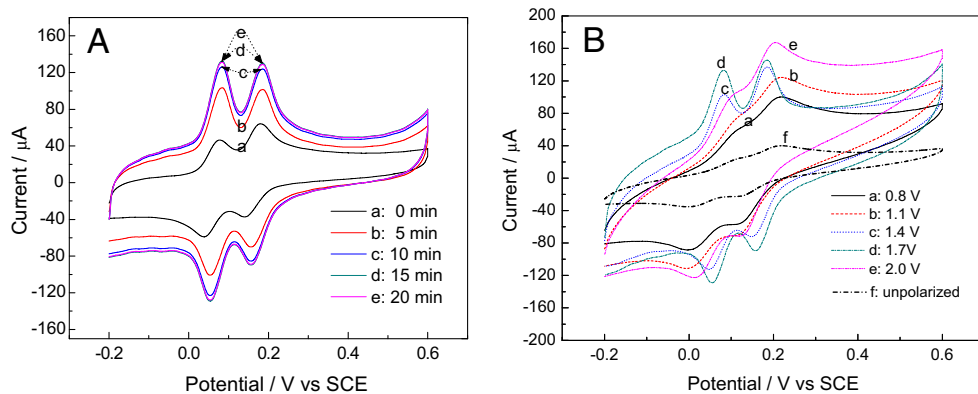
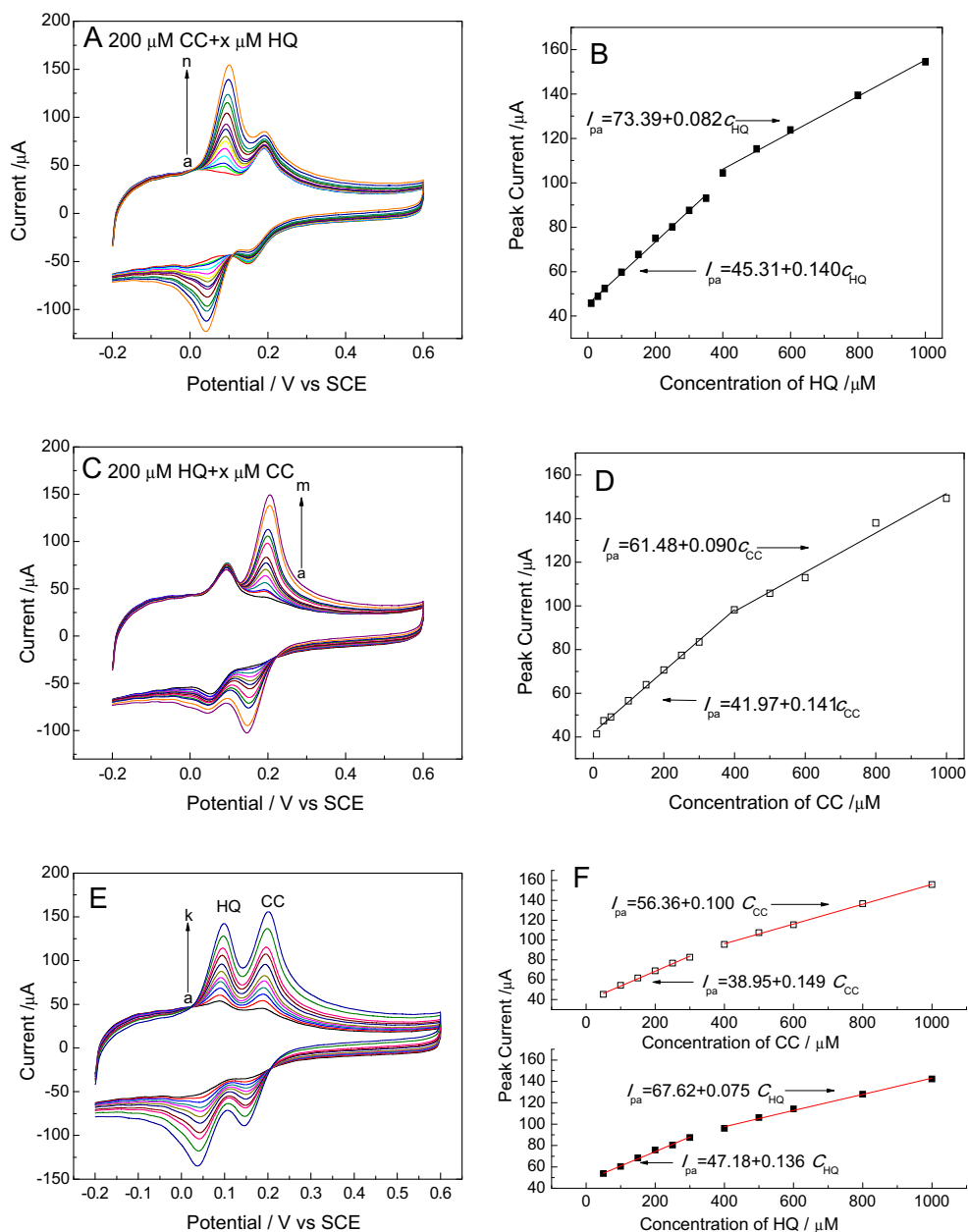


**Fig. 6** A CVs of (a–n) 10, 30, 50, 100, 150, 200, 250, 300, 350, 400, 500, 600, 800, and 1000 μM HQ with constant CC concentration at 200 μM in 0.1 M PBS (pH 7.0) at 50 mV s<sup>-1</sup> scan rate. B Calibration plots of HQ oxidation peak current vs the concentration of HQ. C: CVs of (a–m) 10, 30, 50, 100, 150, 200, 250, 300, 400, 500, 600, 800, and 1000 μM CC with constant HQ concentration at 200 μM in 0.1 M PBS (pH 7.0) at 50 mV s<sup>-1</sup> scan rate. D Calibration plots of CC oxidation peak current vs concentration of CC. E CVs of (a–k) 50, 100, 150, 200, 250, 300, 400, 500, 600, 800, and 1000 μM HQ and CC in 0.1 M PBS (pH 7.0) at 50 mV s<sup>-1</sup> scan rate. F Calibration plots of oxidation peak current vs concentration of HQ and CC, respectively





concentration of the probe molecule, respectively. In  $\text{Fe}(\text{CN})_6^{4-/3-}$  redox system, the  $D$  is equal to  $7.6 \times 10^{-6}$  [41],  $n$  equals 1,  $\nu$  is 0.02 V/s, and  $C$  is 20 mM here. The electroactive surface of unpolarized GCE and PGCE was calculated to be 0.131 and 0.186  $\text{cm}^2$ , respectively. The results indicate that the surface area of PGCE is 1.4 times of the GCE. The results demonstrate that the electrochemical treating GCE by anodizing at 1.7 V for 20 min and then cathodizing at  $-1.0$  V for 15 min could distinctly increase the electron transfer rate of  $\text{Fe}(\text{CN})_6^{3-/4-}$ . In order to further clarify the differences of the electrochemical performance between GCE and PGCE, electrochemical impedance spectroscopy (EIS) was carried out, which can be employed to estimate the interfacial changes in the electrode surface [42]. Figure 4B shows impedance plots for (a) unpolarized GCE and (b) PGCE in 20 mM  $\text{K}_3\text{Fe}(\text{CN})_6/\text{K}_4\text{Fe}(\text{CN})_6$  (1:1) with 0.1 M KCl. The semicircular elements correspond to the charge transfer resistance at the electrode surface [38], and the large diameter from curve a was equivalent to about 1500  $\Omega$  electron transfer resistance for the unpolarized GCE. However, the diameter of the semicircle diminished when PGCE was employed. About 700  $\Omega$

charge transfer resistance can be estimated from the diameter of the curve b, which is one half smaller than that of unpolarized GCE. The charge transfer resistance values obtained from this observation implied that the charge transfer resistance of the electrode surface decreased and the charge transfer rate increased, which confirmed that the polarization mentioned above could effectively increase the electron transfer rate of  $\text{Fe}(\text{CN})_6^{3-/4-}$ .

### Cyclic voltammetry characteristics of HQ and CC

In order to optimize the electrochemical activity of HQ and CC at different polarized electrodes, CV were performed in PBS containing 500  $\mu\text{M}$  HQ and 500  $\mu\text{M}$  CC at the scan rate of 50  $\text{mV s}^{-1}$ . Figure 5A shows the effect of cathodization time on the CV behavior of HQ and CC on the PGCE after anodizing at 1.7 V for 20 min. As shown in Fig. 5A, the peak currents of HQ and CC increase with the cathodization time from 0 (curve a) to 20 min (curve e) and the sensitivity to HQ and CC stops increasing after 15-min cathodization. Figure 5B shows the influence of anodization potential on the property of

**Table 1** Comparison of linear range, sensitivity and detection limit of HQ and CC at the PGCE with previously reported modified GCE by nanocarbon materials

Modifying materials	Method	Linear range of HQ/CC $\mu\text{M}$	Sensitivity of HQ/CC $\mu\text{A}/\mu\text{M}$	Detection limit of HQ/CC $\mu\text{M}$	Ref.
BG <sup>a</sup>	DPV	5–100/1–75	0.2373/0.7673	0.3/0.2	[7]
GR/MWCNTs/BMIMPF <sub>6</sub> <sup>b</sup>	DPV	0.5–465/0.2–80	0.1140/0.2233	0.1/0.06	[8]
CNCs/RGO <sup>c</sup>	DPV	1–400/1–300	0.0726/0.2055	0.87/0.40	[9]
AuNPs/Fe <sub>3</sub> O <sub>4</sub> -APTES-GO <sup>d</sup>	Amperometry	3–137/2–145	0.0020/0.0017	1.1/0.8	[14]
Pt/ZrO <sub>2</sub> -RGO <sup>e</sup>	DPV	1–400/1–1000	0.026/0.017	0.4/0.4	[17]
PEDOT/NGE <sup>f</sup>	DPV	1–10/1–10	0.778/0.556	0.18/0.26	[19]
PANi-Fe <sub>2</sub> O <sub>3</sub> -rGO <sup>g</sup>	DPV	0.1–550/–	0.238/–	0.06/–	[21]
3DFG <sup>h</sup>	DPV	0.31–13.1/0.25–12.9	0.078/0.058	0.10/0.08	[40]
GQD <sup>i</sup>	DPV	4.0–600/6.0–400	0.051/0.069	0.40/0.75	[42]
GMC <sup>j</sup>	DPV	2–50/2–70	1.091/0.439	0.37/0.31	[44]
GO-MnO <sub>2</sub> <sup>k</sup>	DPV	1–10/–	2/–	0.8/–	[45]
TiO <sub>2</sub> /MWCNT <sup>l</sup>	DPV	0.1–100/–	0.21/–	0.04/–	[46]
PGCE	CV	10–300/10–300	0.136/0.149	3.57/3.99	This work

<sup>a</sup> Boron-doped graphene

<sup>b</sup> Graphene/multiwall carbon nanotubes/1-butyl-3-methylimidazolium hexafluorophosphate

<sup>c</sup> Carbon nanocages (CNCs)/Reduced graphene oxides

<sup>d</sup> Fe<sub>3</sub>O<sub>4</sub> functionalized graphene oxide-gold nanoparticle composite

<sup>e</sup> Pt/ZrO<sub>2</sub>/Reduced graphene oxide

<sup>f</sup> Poly(3,4-ethylenedioxythiophene)/nitrogen-doped graphene composite

<sup>g</sup> Polyaniline nanofiber incorporated into iron oxide-reduced graphene oxide

<sup>h</sup> Three-dimensional functionalized graphene

<sup>i</sup> Graphene quantum dots

<sup>j</sup> Graphitic mesoporous carbon

<sup>k</sup> Graphene oxide-mesoporous MnO<sub>2</sub>

<sup>l</sup> TiO<sub>2</sub>/Multiwall carbon nanotubes

PGCE. Note that there was always 15-min cathodization at  $-1.0$  V after the 20-min anodization in Fig. 5B. The results indicate that the anodizing potential has markedly affected the peak current of HQ and CC on the CV curves. The peak currents turn bigger with the increase of anodization potential from 0.8 (curve a) to 2.0 V (curve e).

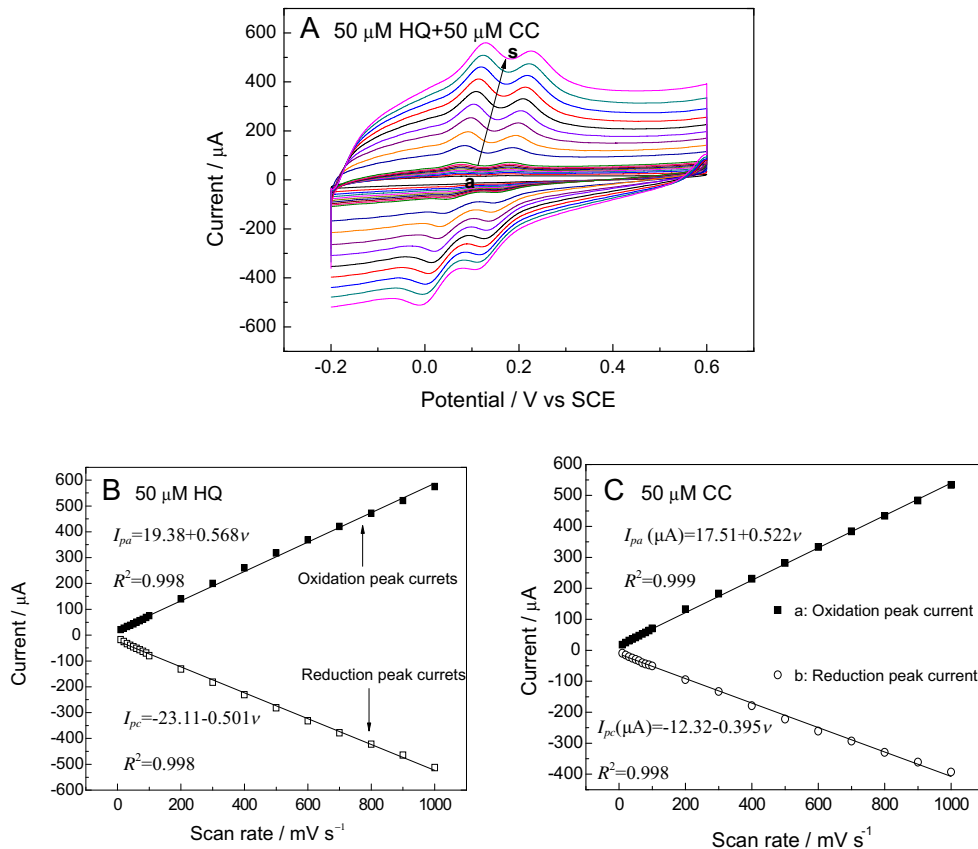
Comparing curve d (PGCE, cathodizing at  $-1.0$  V for 15 min after 20 min anodization) and curve f (unpolarized GCE) in Fig. 5B, two pairs of current peaks are clearly observed at curves d, which show that the oxidation and reduction peaks of HQ and CC can be separated, while on curve f, the oxidation peaks of HQ and CC are not separated clearly. The redox peak potential difference ( $\Delta E_p$ ) of HQ and CC on unpolarized GCE is 0.114 and 0.104 V, respectively, while the  $\Delta E_p$  on PGCE is 0.027 V for HQ and 0.027 V for CC, respectively, indicating a better reversibility [17]. Additionally, the peak currents on PGCE are about five times of that on GCE, showing a better sensitivity to HQ and CC detection. These results suggest that the PGCE can not only differentiate the HQ and CC, but also greatly enhance their detection sensitivity by a simple treatment of electrochemical polarization. Considering the selective and simultaneous determination of HQ and CC, the optimal conditions for anodization and cathodization of the GCE in PBS are 1.7 V for 20 min and then  $-1.0$  V for 15 min.

### Simultaneous determination of HQ and CC

Based on the experiments mentioned above, CV method was used in simultaneous determination of HQ and CC in 0.1 M PBS (pH 7.0) at  $50$   $\text{mV s}^{-1}$  scan rate. Three conditions were studied in determination of HQ and CC. (i) Concentration of CC was kept constant at  $200$   $\mu\text{M}$ ; HQ was added in pH 7 PBS from 10 to  $1000$   $\mu\text{M}$  (curve a–n), as shown in Fig. 6A. (ii) Concentration of HQ was kept constant at  $200$   $\mu\text{M}$ ; CC was added in pH 7 PBS from 10 to  $1000$   $\mu\text{M}$  (curve a–m), as shown in Fig. 6C. (iii) HQ and CC were added simultaneously in pH 7 PBS from 10 to  $1000$   $\mu\text{M}$  (curve a–k), as shown in Fig. 6E.

As shown in Fig. 6A, C, and E, the peak currents of the CVs increase with the increasing of the analytes concentration. In addition, the peaks of HQ and CC show a good separation. Figure 6B, D, and F show the relationship between the analytes oxidation peak currents and their concentrations. Relative linear regression equations have been marked in the figures with formula. It can be seen that the peak currents of the analytes are linear to the concentration of the analytes in two regions. The sensitivity to HQ in Fig. 6B at low concentration region is  $0.140$   $\mu\text{A}/\mu\text{M}$ , which is in accordance with the  $0.136$   $\mu\text{A}/\mu\text{M}$  sensitivity to HQ in Fig. 6E. The sensitivity to CC in Fig. 6D at low concentration region is  $0.141$   $\mu\text{A}/\mu\text{M}$ , which is in accordance with the  $0.149$   $\mu\text{A}/$

**Fig. 7** **A:** CVs of  $50$   $\mu\text{M}$  HQ and CC at scan rate of (a–s)  $10$ – $1000$   $\text{mV s}^{-1}$ . **B:** The redox peak currents of HQ vs scan rate. **C:** The redox peak currents of CC vs scan rate



$\mu\text{M}$  sensitivity to CC in Fig. 6E. The limit of detection (LOD) to HQ and CC is 3.57 and 3.99  $\mu\text{M}$  (3S/N), respectively, and the limit of quantitation (LOQ) to HQ and CC is 11.90 and 13.30  $\mu\text{M}$  (10S/N) [43]. These results indicate that the two isomers of dihydroxybenzene can be differentiated on the PGCE from the redox peaks on the CV curves. Thus, this proposed method allows us to detect HQ and CC simultaneously and sensitively without interference with each other. The comparison of this facile method of electrochemical disposed PGCE in simultaneous detection of HQ and CC with other literatures of nanocarbon materials modified GCE is listed in Table 1.

It can be seen that the sensitivity of the PGCE can be compared with the most reported nanocarbon materials modified electrodes. Although the LOD are not as good as the reported literatures, it is enough in environment pollution detection. The advantages of the proposed method against the other methods in Table 1 reflect its facile and green electrochemical treatment, low cost, highly sensitive, stable, and reproducible of the glassy carbon electrode based sensor for electrochemical sensing of HQ and CC.

Although the PGCE is verified in simultaneous detection of HQ and CC at low concentrations, it is still necessary to explain the segmented sensitivity in different concentrations. Generally, sensitivity segmentation is mostly owing to the conversion of the rate-determine step of the electrochemical reaction that occurs at the electrode [47]. Thus, reaction kinetic of HQ and CC on the PGCE was studied by the effect of CV scan rate on the peak current of HQ and CC. Concerning the sensitivity segment occurs at different concentrations, two concentrations (50 and 1000  $\mu\text{M}$ ) of HQ and CC solution were investigated.

At low concentration of 50  $\mu\text{M}$  HQ and 50  $\mu\text{M}$  CC in 0.1 M PBS (pH 7.0), CVs on the PGCE at different scan rates are shown in Fig. 7A. As can be seen, the oxidation peak currents and reduction peak currents for HQ and CC increase regularly with the increase of scan rates from 10 to 1000  $\text{mV s}^{-1}$  (curve a–s). However, with the increase of scan rate, especially in the range of high scan rate, the oxidation peak potential shifted positively and the reduction peak potential shifted negatively, which suggests that the redox reversibility of HQ and CC was impaired at high scan rate [48].

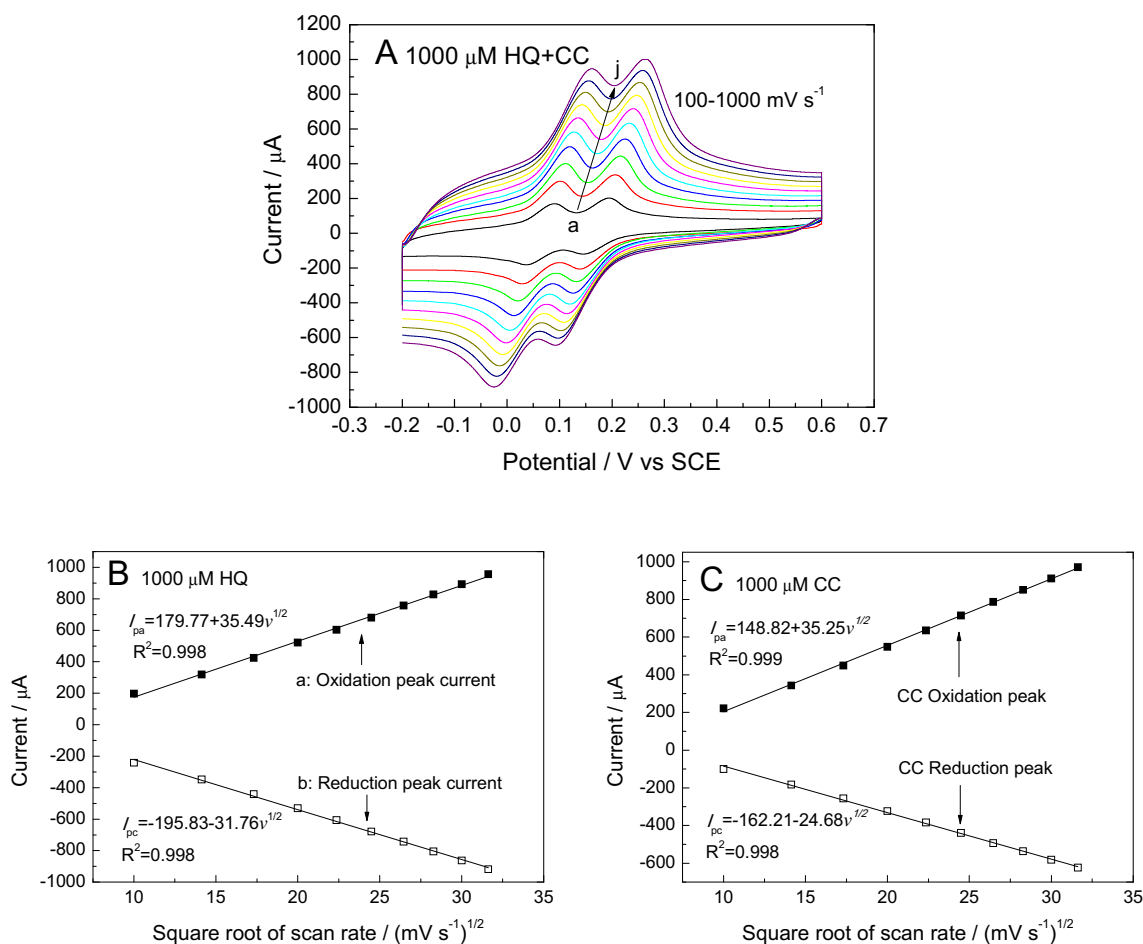


**Fig. 8** A CVs of 1000  $\mu\text{M}$  HQ and 1000  $\mu\text{M}$  CC at scan rate of (a–j) 100, 200, 300, 400, 500, 600, 700, 800, 900, and 1000  $\text{mV s}^{-1}$ . B The HQ redox peak currents vs square root of scan rate. C The CC redox peak currents vs square root of scan rate



Figure 7B and C present the plots of the oxidation peak currents and reduction peak currents of HQ and CC against the scan rates. It is clear that the redox peak currents are in linear relationship to the scan rates. As known, linear relationship between scan rate and peak currents is the character of surface adsorption control process [44].

At a high concentration of 1000  $\mu\text{M}$ , the effect of scan rate (a–j: 100–1000  $\text{mV s}^{-1}$ ) on the CVs of a mixed solution of 1000  $\mu\text{M}$  HQ and 1000  $\mu\text{M}$  CC in 0.1 M PBS (pH 7.0) at PGCE are shown in Fig. 8A. The results show that the anodic peak currents and cathodic peak currents are in linear relationship with the square root of the scan rates and relative equations have been marked in Fig. 8B and C, which indicate that the electrode reactions of HQ and CC at PGCE are typical diffusion-controlled process at the high concentration. In addition, with the increase of scan rate, the oxidation peak potentials of HQ and CC shifted positively and the opposite reduction peak potentials shifted negatively, which is in accordance with the reported literature [49], suggesting that reversibility of the redox was also impaired at high scan rate.

In summary, electrochemical redox reactions of HQ and CC at the PGCE are heterogeneous and the kinetics are not only depended on the properties of the electrode/electrolyte interface but also related to the concentration of reactant. A surface adsorption control process at low concentration might convert into a diffusion-controlled process at high concentration. The conversion in rate-determine steps could offer a support to the segmented sensitivity in detection of HQ and CC as shown in Fig. 6B, D, and F.

### Reproducibility and repeatability

The reproducibility and repeatability are important parameters for the evaluation of the sensor performance. The reproducibility of PGCE was estimated from the CV response to 150  $\mu\text{M}$  HQ and CC for five PGCEs prepared under the same experiment conditions. The relative standard deviation was found to be 3.89 and 3.97 % for HQ and CC, respectively, indicating a good reproducibility of the electrochemical treatment technique. The repeatability of PGCE was also examined by monitoring the CV response to 150  $\mu\text{M}$  HQ and CC for ten successive measurements using the same electrode. The relative standard deviation was found to be 1.83 and 2.02 % for HQ and CC, respectively. The results indicate that the proposed PGCE has very good reproducibility and repeatability in simultaneous detection of HQ and CC.

### Conclusion

Glassy carbon electrodes have been electrochemically polarized for simultaneous detection of HQ and CC by cyclic voltammetry measurement. The optimized polarization is anodizing at

1.70 V for 20 min and cathodizing at  $-1.0$  V for 15 min successively in 0.1 M pH 7.0 PBS. After polarization disposal, abundant carboxyl and hydroxyl generate on the surface of PGCE. The electrochemical reaction kinetic of HQ and CC on the PGCE converts from surface adsorption control process to diffusion-controlled process from low concentration to high concentration. The linear range in detection of HQ and CC is both 10–300  $\mu\text{M}$  and the limit of detection (LOD) to HQ and CC is 3.57 and 3.99  $\mu\text{M}$ , respectively. The proposed method has advantage of simple, stable and low cost by the green electrochemical treatment of the glassy carbon electrode for electrochemical sensing of HQ and CC.

**Acknowledgments** This work was supported by the National Natural Science Foundation of China (No: 21405096) and University Student Innovation Training Project of China (No: 201510445111; 201510445122).

### References

- Hong Z, Zhou L, Li J, Tang J (2013) A sensor based on graphitic mesoporous carbon/ionic liquids composite film for simultaneous determination of hydroquinone and catechol. *Electrochim Acta* 109:671–677
- Buleandra M, Rabinca AA, Mihailciuc C, Balan A, Nichita C, Stamatini I, Ciucu AA (2014) Screen-printed prussian blue modified electrode for simultaneous detection of hydroquinone and catechol. *Sensors Actuators B Chem* 203:824–832
- Marrubini G, Calleri E, Coccini T, Castoldi AF, Manzo L (2005) Direct analysis of phenol, catechol and hydroquinone in human urine by coupled-column HPLC with fluorimetric detection. *Chromatographia* 62:25–31
- Wittig J, Wittmer S, Veit M (2001) Validated method for the determination of hydroquinone in human urine by high-performance liquid chromatography-coulometric-array detection. *J Chromatogr B* 761:125–132
- Li J, Liu CY, Cheng C (2011) Electrochemical detection of hydroquinone by graphene and Pt-graphene hybrid material synthesized through a microwave-assisted chemical reduction process. *Electrochim Acta* 56:2712–2716
- Tehrani RMA, Ghadimib H, Ghani SA (2013) Electrochemical studies of two diphenols isomers at graphene nanosheet-poly(4-vinyl pyridine) composite modified electrode. *Sensors Actuators B Chem* 177:612–619
- Zhang Y, Sun R, Luo B, Wang L (2015) Boron-doped graphene as high-performance electrocatalyst for the simultaneous electrochemical determination of hydroquinone and catechol. *Electrochim Acta* 156:228–234
- Wang X, Wu M, Li H, Wang Q, He P, Fang Y (2014) Simultaneous electrochemical determination of hydroquinone and catechol based on three-dimensional graphene/MWCNTs/BMIMPF<sub>6</sub> nanocomposite modified electrode. *Sensors Actuators B Chem* 192:452–458
- Huang YH, Chen JH, Sun X, Su ZB, Xing HT, Hu SR, Weng W, Guo HX, Wu WB, He YS (2015) One-pot hydrothermal synthesis carbon nanocages-reduced graphene oxide composites for simultaneous electrochemical detection of catechol and hydroquinone. *Sensors Actuators B Chem* 212:165–173
- Erogul S, Bas SZ, Ozmen M, Yildiz S (2015) A new electrochemical sensor based on Fe<sub>3</sub>O<sub>4</sub> functionalized graphene oxide-gold

- nanoparticle composite film for simultaneous determination of catechol and hydroquinone. *Electrochim Acta* 186:302–313
11. Liu H, Chen Y, Liu Y, Yang Z (2013) A sensitive sensor for determination of L-tryptophan based on gold nanoparticles/poly(alizarin red S)-modified glassy carbon electrode. *J Solid State Electrochem* 17:2623–2631
  12. Vilian ATE, Chen SM, Huang LH, Ali MA, Al-Hemaid FMA (2014) Simultaneous determination of catechol and hydroquinone using a Pt/ZrO<sub>2</sub>-RGO/GCE composite modified glassy carbon electrode. *Electrochim Acta* 125:503–509
  13. Si W, Lei W, Han Z, Hao Q, Zhang Y, Xia M (2014) Selective sensing of catechol and hydroquinone based on poly(3,4-ethylenedioxythiophene)/nitrogen-doped graphene composites. *Sensors Actuators B Chem* 199:154–160
  14. Radhakrishnan S, Krishnamoorthy K, Sekar C, Wilson J, Kim SJ (2015) A promising electrochemical sensing platform based on ternary composite of polyaniline-Fe<sub>2</sub>O<sub>3</sub>-reduced graphene oxide for sensitive hydroquinone determination. *Chem Eng J* 259:594–602
  15. Shahrokhian S, Zare-Mehrjardi HR, Khajehsharifi H (2009) Modification of carbon paste with congo red supported on multi-walled carbon nanotube for voltammetric determination of uric acid in the presence of ascorbic acid. *J Solid State Electrochem* 13:1567–1575
  16. Liu X, Li Y, Liu X, Zeng X, Kong B, Luo S, Wei W (2012) Simple sensor for simultaneous determination of dihydroxybenzene isomers. *J Solid State Electrochem* 16:883–889
  17. Wang L, Zhang Y, Du Y, Lu D, Zhang Y, Wang C (2012) Simultaneous determination of catechol and hydroquinone based on poly (diallyldimethylammonium chloride) functionalized graphene-modified glassy carbon electrode. *J Solid State Electrochem* 16:1323–1331
  18. Dong S, Zhang P, Yang Z, Huang T (2012) Simultaneous determination of catechol and hydroquinone by carbon paste electrode modified with hydrophobic ionic liquid-functionalized SBA-15. *J Solid State Electrochem* 16:3861–3868
  19. Li SJ, Xing Y, Deng DH, Shi MM, Guan PP (2015) A comparative study of different types of reduced graphene oxides as electrochemical sensing platforms for hydroquinone and catechol. *J Solid State Electrochem* 19:861–870
  20. Zhou S, Wu H, Wu Y, Shi H, Feng X, Huang H, Li J, Song W (2013) Large surface area carbon material with ordered mesopores for highly selective determination of l-tyrosine in the presence of l-cysteine. *Electrochim Acta* 112:90–94
  21. Walcarius A (2012) Electrocatalysis, sensors and biosensors in analytical chemistry based on ordered mesoporous and macroporous carbon-modified electrodes. *Trends Anal Chem* 38:79–97
  22. Hasoň S, Vetterl V, Jelen F, Fojta M (2009) Improved sensitivity and selectivity of uric acid voltammetric sensing with mechanically grinded carbon/graphite electrodes. *Electrochim Acta* 54:1864–1873
  23. Zittel HE, Miller FJ (1965) A glassy-carbon electrode for voltammetry. *Anal Chem* 37:200–203
  24. Stutts KJ, Kovach PM, Kuhr WG, Wightmen RM (1983) Enhanced electrochemical reversibility at heat-treated glassy carbon electrodes. *Anal Chem* 55:1632–1634
  25. Gu H, Xu Y, Peng W, Li G, Chen HY (2004) A novel method for separating the anodic voltammetric peaks of dopamine and ascorbic acid. *Microchim Acta* 146:223–227
  26. Kuo TC, McCreery RL (1999) Surface chemistry and electron-transfer kinetics of hydrogen-modified glassy carbon electrodes. *Anal Chem* 71:1553–1560
  27. Poon M, McCreery RL, Engstrom R (1988) Laser activation of carbon electrodes. Relationship between laser-induced surface effects and electron transfer activation. *Anal Chem* 60:1725–1730
  28. DeClements R, Swain GM, Dallas T, Holtz MW, Herrick RD II, Stickney JL (1996) Electrochemical and surface structural characterization of hydrogen plasma treated glassy carbon electrodes. *Langmuir* 12:6578–6586
  29. Wang J, Lin MS (1988) *In situ* electrochemical renewal of glassy carbon electrodes. *Anal Chem* 60:499–502
  30. Dai HP, Shiu KK (1996) Voltammetric studies of electrochemical pretreatment of rotating-disc glassy carbon electrodes in phosphate buffer. *J Electroanal Chem* 419:7–14
  31. Ilangoan G, Chandrasekara Pillai K (1999) Mechanism of activation of glassy carbon electrodes by cathodic pretreatment. *J Solid State Electrochem* 3:357–360
  32. Huang D, Cheng Y, Xu H, Zhang H, Sheng L, Xu H, Liu Z, Wu H, Fan S (2015) The determination of uric acid in human body fluid samples using glassy carbon electrode activated by a simple electrochemical method. *J Solid State Electrochem* 19:435–443
  33. Ahammad AJS, Sarker S, Rahman MA, Lee JJ (2010) Simultaneous determination of hydroquinone and catechol at an activated glassy carbon electrode. *Electroanalysis* 22:694–700
  34. Shi K, Shiu KK (2004) Adsorption of some quinone derivatives at electrochemically activated glassy carbon electrodes. *J Electroanal Chem* 574:63–70
  35. Yang Y, Lin ZG (1995) *In situ* FTIR characterization of the electrooxidation of glassy carbon electrodes. *J Appl Electrochem* 25:259–266
  36. Du W, Zhou B, Jiang X (2014) Fast electron transfer kinetics on electrodes composed of graphene oxide ‘patched’ with direct exfoliated pristine graphene nanosheets. *Chem Phys Lett* 595-596:1–5
  37. Ranganathan S, Kuo TC, McCreery RL (1999) Facile preparation of active glassy carbon electrodes with activated carbon and organic solvents. *Anal Chem* 71:3574–3580
  38. Li F, Song J, Gao D, Zhang Q, Han D, Niu L (2009) Simple and rapid voltammetric determination of morphine at electrochemically pretreated glassy carbon electrodes. *Talanta* 79:845–850
  39. Gao H, Sun Y, Zhou J, Xu R, Duan H (2013) Mussel-inspired synthesis of polydopamine-functionalized graphene hydrogel as reusable adsorbents for water purification. *Appl Mater Interfaces* 5:425–432
  40. Du J, Ma L, Shan D, Fan Y, Zhang L, Wang L, Lu X (2014) An electrochemical sensor based on the three-dimensional functionalized graphene for simultaneous determination of hydroquinone and catechol. *J Electroanal Chem* 722-723:38–45
  41. Fu L, Lai G, Jia B, Yu A (2015) Preparation and electrocatalytic properties of polydopamine functionalized reduced graphene oxide-silver nanocomposites. *Electrocatalysis* 6:72–76
  42. Jian X, Liu X, Yang HM, Guo MM, Song XL, Dai HY, Liang ZH (2016) Graphene quantum dots modified glassy carbon electrode via electrostatic self-assembly strategy and its application. *Electrochim Acta* 190:455–462
  43. Uhrovčík J (2014) Strategy for determination of LOD and LOQ values – Some basic aspects. *Talanta* 119:178–180
  44. Yuan X, Yuan D, Zeng F, Zou W, Tzorbatozoglou F, Tsiakaras P, Wang Y (2013) Preparation of graphitic mesoporous carbon for the simultaneous detection of hydroquinone and catechol. *Appl Catal B Environ* 129:367–374
  45. Gan T, Sun J, Huang K, Song L, Li Y (2013) A graphene oxide-mesoporous MnO<sub>2</sub> nanocomposite modified glassy carbon electrode as a novel and efficient voltammetric sensor for simultaneous determination of hydroquinone and catechol. *Sensors Actuators B Chem* 177:412–418
  46. Meng Z, Zhang H, Zheng J (2015) An electrochemical sensor based on titanium oxide-carbon nanotubes nanocomposite for simultaneous determination of hydroquinone and catechol. *Res Chem Intermed* 41:3135–3146
  47. Nematollahi D, Ariapad A, Rafiee M (2007) Electrochemical nitration of catechols: Kinetic study by digital simulation of cyclic voltammograms. *J Electroanal Chem* 602:37–42

48. Song D, Xia J, Zhang F, Bi S, Xiang W, Wang Z, Xia L, Xia Y, Li Y, Xia L (2015) Multiwall carbon nanotubes-poly(diallyldimethylammonium chloride)-graphene hybrid composite film for simultaneous determination of catechol and hydroquinone. *Sensors Actuators B Chem* 206:111–118
49. Zhang Y, Zheng JB (2007) Comparative investigation on electrochemical behavior of hydroquinone at carbon ionic liquid electrode, ionic liquid modified carbon paste electrode and carbon paste electrode. *Electrochim Acta* 52: 7210–7216